Density-Adaptive and Geometry-Aware Registration of TLS Point Clouds Based on Coherent Point Drift

Zang, Yufu; Lindenbergh, Roderik; Yang, Bisheng; Guan, Haiyan

DOI
10.1109/LGRS.2019.2950128

Publication date
2020

Document Version
Accepted author manuscript

Published in
IEEE Geoscience and Remote Sensing Letters

Density adaptive and geometry aware registration of TLS point clouds based on Coherent Point Drift

Yufu Zang[*1,2], Roderik Lindenbergh[#2], Bisheng Yang[#3], Haiyan Guan[#1]

***Abstract*—Probabilistic registration algorithms (e.g. Coherent Point Drift, CPD) provide effective solutions for point cloud alignment. However, using the original CPD algorithm for automatic registration of Terrestrial Laser Scanner (TLS) point clouds is highly challenging because of density variations caused by scanning acquisition geometry. In this paper, we propose a new global registration method introducing the use of the CPD framework for TLS point clouds. We first consider the measurement geometry and the intrinsic characteristics of the scene to simplify points. In addition to the Euclidean distance, we then incorporate geometric information as well as structural constraints in the probabilistic model to optimize the so-called matching probability matrix. Among the structural constraints, we use a spectral graph to measure the structural similarity between matches at each iteration. The method is tested on three datasets collected by different TLS scanners. Experimental results demonstrate that the proposed method is robust to density variations, and can decrease iterations effectively. The average registration errors of the three datasets are 0.05m, 0.12m, and 0.08m, respectively. It is also shown that our registration framework is superior to state-of-the-art methods in terms of both registration errors and efficiency. The experiments demonstrate the effectiveness and efficiency of the proposed probabilistic global registration.**

***Index Terms*—Coherent Point Drift, density variations, global registration, matching probability matrix, structural constraints.**

I. Introduction

TLS technique has been used in a variety of applications including cultural heritage documentation, urban planning, terrain deformation monitoring as well as forest biomass estimation [1-2]. TLS point cloud registration which aligns scans from multiple stations in a common 3D coordinate system is critical to the above applications.

Various registration methods have been explored. According to the strategy of correspondence search, existing registration methods are categorized into: local and global registration methods [3].The proposed approach falls into the latter group.

Local registration methods determine point correspondences locally between adjacent stations. It begins with a proper initialized alignment and does not account for any neighborhood coherency. The Iterative Closest Point (ICP) algorithm [4-5] is probably the most well-known local method, which seeks the closest points as point correspondence and minimizes the sum of squared differences in an iterative way. Various ICP variants have also been proposed [6-7]. In addition, the *Normal Distribution Transform* (NDT), the *Support Vector Registration* (SVR) algorithm, and the *simultaneous localization and mapping* (SLAM) algorithms have also been introduced for local point cloud registration [8-10]. Nevertheless, these approaches still rely on sufficient initialization or are vulnerable to convergence to local minima, which limit their applications in practice.

Global registration methods regard all points as candidates, and determine correspondences globally, which is needed in case of a large transformation or when small overlap exists. Geometric primitive based methods extract geometric features (e.g., key points, straight lines, spatial curves, planes, curved surfaces) first, use local descriptors (e.g., spin image, shape context, curvature, covariance matrix, FPFH) to describe their geometric characteristics, and determine the corresponding primitives globally [11-12]. However, these methods rely on the accurate extraction of geometric primitives. There is another line of work focusing on the matching strategy including Random sample consensus (RANSAC) [13], and the 4-points Congruent Sets (4PCS) algorithm [14].

Motivated by the limitations of existing methods, several probabilistic registration methods have been explored. The CPD algorithm [15] is one of most popular methods because of its generality and accuracy [16], which considers registration as an estimation problem of probability density. It fits Gaussian Mixed Models (GMM) centroids to point clouds by maximizing the likelihood of probability. On this basis, Wang *et al.* [17] introduced a new parameter for outlier modeling. Peng *et al.* [18] used shape context to describe local geometric information, increasing its robustness. In addition, Lawin *et al.* [19] used hyper-parameters to weigh points to incorporate the effect of density variation, which works well for small-scale indoor scenes. However, some drawbacks still exist. For data with density variations, the registration easily converges to a local extremum (as Figure 1 shows), and the robustness and efficiency should also be improved. These problems become even more challenging when working on TLS point clouds, as these always have density variations because of the scanning acquisition geometry [20].

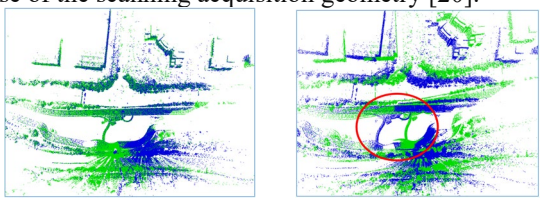

Figure 1. Two alignment results for TLS point clouds with varying density: (a) Correct alignment result; (b) Alignment by state-of-the-art probability method;

Considering the above limitations, we propose a density adaptive CPD algorithm using geometric information and structural constraints for TLS point cloud registration. This algorithm is based on one reasonable assumption, that levelling was performed before scanning, which means that

rotations only occur within the horizontal plane between TLS stations. This paper has two major contributions.

(1)We propose an approximately uniform sampling method by considering the measurement geometry and the intrinsic characteristics of scene to reduce the influence of density variations;

(2)In the probability model, we show how to incorporate the geometric information and structural constraints. The structural similarity of each iteration optimizes the matching probability matrix, improving the robustness and efficiency.

The rest of this letter is organized as: Section Ⅱ introduces the approximately uniform simplification, a probabilistic registration method considering the geometric constraints, and the structural similarity. Section Ⅲ presents the experimental results on real datasets. Section Ⅳ concludes this letter.

II. DENSITY ADAPTIVE PROBABILISTIC FRAMEWORK

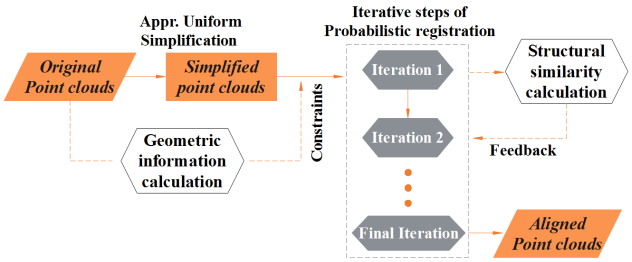

Figure 2. Pipeline of the proposed method.

The pipeline of the proposed registration method is sketched in Figure 2. It contains three main components, namely: (1) approximately uniform sampling of input point clouds; (2) probabilistic registration method based on geometric constraints; (3) improvement by static and dynamic structural information. The three components are described in detail in the following sections.

A. Approximately Uniform Simplification

The probabilistic registration method takes the sum of matching probabilities as its objective value, leading to its sensitivity to point density variations. To mitigate this influence, we propose to apply a sampling algorithm before probabilistic registration is performed.

The algorithm consists of an importance score and an iterative strategy to successively reduce points. The importance score of each point is calculated by considering its local intrinsic characteristics and the measurement geometry. First we evaluate the score of each point, eliminate the least important points, and update the score of its neighbors. Finally, we repeat this procedure until the required number of points is obtained. The score w_i of each point is calculated as,

$$\begin{cases} w_i = w_g \cdot w_m \\ w_g = \dfrac{Cur_i}{1 + a \cdot density_i}, w_m = \dfrac{\exp(b \cdot R_i)}{1 + \exp(\vec{n_i} \cdot \vec{x_{io}})} \end{cases} \quad (1)$$

Here, w_g is the weight of the local intrinsic characteristics, and w_m describes the weight of the measurement geometry. Cur_i is the curvature of point i, $density_i$ is the number of neighbors. R_i is the distance between point i and the scanner center, $\vec{n_i}$ is the normal vector of point i, and $\vec{x_{io}}$ is the direction from point i to the scanner center. a and b are weight coefficients used to balance these two terms (e.g., a=300.0, b=0.02). To improve robustness, we used [21] to select optimal neighbourhood size for each point. In addition, we applied a weighting method [22] and fitting method [23] to estimate normals and curvatures, respectively.

According to Formula 1, the scores of points in flat and densely sampled areas are decreased. Thus, we obtain an approximately uniform sampling result, and reduce density variations. Besides, during the estimation of normal vectors, noise can be detected and suppressed as well.

B. Probabilistic Registration with Geometric Constraints

According to the CPD algorithm [15], for two point clouds X and Y, the points from X are regarded as the centroids of Gaussian Mixed Models (GMMs), and the points from Y are regarded as the points generated by the GMMs. A probability is calculated to measure the similarity between two points. Y will be aligned with X when the registration probability is maximal. To simplify calculations, an objective function is formed as:

$$\mathrm{E}(\theta, \sigma^2) = -\sum_{n=1}^{N} \log\left[w\frac{1}{N} + (1-w)\sum_{m=1}^{M} P(m)\, p(x_n \mid m) \right] \quad (2)$$

Here, $0 \le w \le 1$ indicates the fraction of noise or outliers. N and M are the number of points in X and Y, respectively. $P(m)$ is the probability of the m-th GMM component, $p(x_n \mid m)$ indicates the probability that point x_n belongs to the m-th GMM component. To simplify it further, an upper bound is estimated to get a new objective function, written as:

$$Q(\theta, \sigma^2) = \frac{1}{2\sigma^2}\sum_{n=1}^{N}\sum_{m=1}^{M} P^{old}(m \mid x_n) \cdot \left\| x_n - T(y_m) \right\|^2 + \frac{N_P D}{2} \cdot \log \sigma^2 \quad (3)$$

Here, σ^2 is the variance of all GMMs, $P^{old}(m \mid x_n)$ is the posterior probability of the m-th GMM component calculated using the previous parameter values. $T(y_m)$ denotes the transform of y_m, D is the dimensionality of point (D = 3), and N_P is the summation of $P^{old}(m \mid x_n)$.

In Formula 3, to improve the robustness and efficiency of matching, we incorporated geometric information and structural constraints as discussed in *Section C* to estimate the posterior probability $P^{old}(m \mid x_n)$, written as,

$$\begin{cases} P^{old}(m \mid x_n) = \dfrac{q_{x_n, y_m}}{(2\pi\sigma^2)^{D/2}\dfrac{w}{1-w}\dfrac{M}{N} + \sum_{k=1}^{M} q_{x_n, y_k}} \\ q_{x_n, y_m} = \exp\left[-\dfrac{\left\| x_n - T(y_m) \right\|^2}{2\sigma^2} - g_{x_n, y_m} \right] \end{cases} \quad (4)$$

Here, q_{x_n, y_m} is the matching probability of x_n and y_m, g_{x_n, y_m} represents the constraints on curvature and direction, written as,

$$g(x_n, y_m) = \begin{cases} 0 & ,if\ \vec{n}_{x_n} \cdot T(\vec{n}_{y_m}) < 0 \\ w_1\left[1 - \vec{n}_{x_n} \cdot T(\vec{n}_{y_m})\right] + w_2\left|c_{x_n} - c_{y_m}\right| & , else \end{cases} \quad (5)$$

Here $T(\vec{n}_{y_m})$ represents the normal vector of y_m transformed by the transformation of the current iteration, c_{x_n}, c_{y_m} are the curvatures of x_n and y_m, while w_1, w_2 are the weights to balance the geometric constraints (w_1=8.0, w_2=-5.0 are suggested). After the construction of objective function, rotation matrix R and translation vector T are obtained by maximizing Formula 3. Based on the transformation of the last iteration and the constraint conditions, a new objective function is constructed. The above steps are iterated until the transformation becomes stable.

C. Improvement by Static and Dynamic Structures

Local structural information between neighbourhood points is stable and useful to improve correspondences. To quantity it, for each point, we calculate the mean value and variance of curvature within a certain radius. We regard the similarity of this static structure as a prior to update the matching probability. Specifically, the matching probability of x_n and y_m in Formula 4 is improved by a term $s(x_n, y_m)$,

$$q(x_n, y_m) = q(x_n, y_m) \cdot s(x_n, y_m)$$
$$s(x_n, y_m) = \begin{cases} 0, if\ \left|M_n - M_m\right| > T_1\ or\ \left|V_n - V_m\right| > T_2 \\ 1, otherwise \end{cases} \quad (6)$$

Here, M and V are the mean value and variance of curvature, T_1 and T_2 are thresholds (T_1 = 0.07, T_2 = 0.07 are suggested). Note that in this formulation, we assign the probability of two points to be zero if they have large structural difference to improve correspondences.

Based on the matching result of each iteration, we use the spectral graph method proposed in [24] to describe dynamic structural information. For efficiency, after each iteration, the n (such as: 500) correspondences with highest matching probability are taken into consideration. For each scan, we construct a Laplacian matrix to describe the topology (i.e., directions and distances) between points. After SVD decomposition, the structural information is included in the matrix U. We select the first k columns of U (e.g., k=20) to construct an embedded space U^k. The structure of each point is now expressed by each row vector of U^k. For each correspondence (e.g., x_n, y_m) from n selected correspondences, the matching probability is improved by the correlation coefficient $d(x_n, y_m)$ between their row vectors $x_{1\times k}$ and $y_{1\times k}$ as:

$$d(x_n, y_m) = \frac{k\sum_{i=1}^{k} x_i y_i - \sum_{i=1}^{k} x_i \sum_{i=1}^{k} y_i}{\sqrt{k\sum_{i=1}^{k} x_i^2 - \left(\sum_{i=1}^{k} x_i\right)^2}\sqrt{k\sum_{i=1}^{k} y_i^2 - \left(\sum_{i=1}^{k} y_i\right)^2}} \quad (7)$$

$$q(x_n, y_m) = q(x_n, y_m) \cdot d(x_n, y_m), d(x_n, y_m) = \begin{cases} 0, if\ d(x_n, y_m) < T \\ 1, otherwise \end{cases}$$

T is a threshold (T = 0.5 is suggested).Then the dynamic structure of each iteration is recorded, avoiding convergence to a local extremum, and decreasing the number of iterations.

III. EXPERIMENTAL RESULTS AND ANALYSES

To evaluate performance, the proposed method was evaluated on three sets of TLS point clouds and compared to other state-of-the-art methods including the original CPD algorithm [15], and SC-CPD (shape context based CPD) [18]. Experimental datasets are benchmark data from kos.informatik.uniosnabrueck.de/3Dscans/ or used control targets for validation. TABLE I shows the description of the datasets.

TABLE I
DESCRIPTION OF DATASETS

Dataset	Beach data	Suburb data	Benchmark
Scanner	Leica P40	Riegl VZ-400	Riegl VZ-400
Points Num. T1, T2	391851 336655	514218 508244	260274 267317
Avg. Point Spacing (m)	0.12	0.13	0.26
Overlap Ratio (%)	83.5	61.7	82.9
Characteristics	Flat and rare geometric features	Chaotic forest area and regular urban scene	Disordered points of dock environment

A. Simplification Results

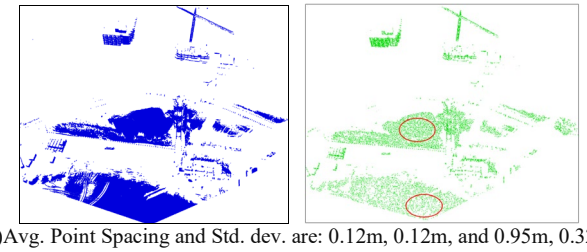

(a)Avg. Point Spacing and Std. dev. are: 0.12m, 0.12m, and 0.95m, 0.32m, respectively.

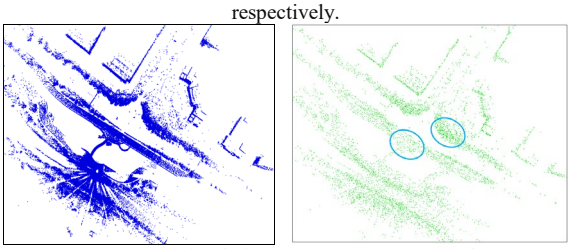

(b)Avg. Point Spacing and Std. dev. are: 0.13m, 0.49m, and 3.28m, 1.68m, respectively.

Figure 3. Initial point clouds (blue) and simplification results (green): (a) Beach data; (b) Suburb data.

We conducted the proposed simplification algorithm on the datasets, and kept about 10,000 points of each point cloud. The simplified results are shown in Figure 3 (here a=10.0, b=0.1 are used). The Avg. Point Spacing and Std. dev. of initial and simplified point clouds are also provided to show the quantitative information of distribution.

Figure 3 shows that severe density variation exist in the initial point clouds. The simplified results and quantitative information demonstrate that the simplified points are more uniformly distributed, and that density variations have been reduced effectively. The red ellipses in Figure 3(a) illustrate that points near the scanner are simplified more. This is because the measurement geometry w_g is considered, balancing the matching probabilities of the areas at different distances. The blue ellipses in Figure 3(b) show that more points are kept in feature rich areas. Because the intrinsic characteristics are weighted by w_m, the sampled points are more descriptive. Compared to the existing methods, we

incorporate both the measurement geometry and the intrinsic characteristics of the scene, making the simplified point clouds more suitable for probabilistic registration.

B. Evaluation of Registration Results

The registration performance of the three datasets is shown in Figure 4 and TABLE II. The registration errors in Figure 4 are evaluated by the distance between closest points in overlapping areas. The registration errors in TABLE Ⅱ are calculated by control targets or benchmark. Avg. error and RMSE indicate the average distance error and mean square root between correspondences. "ablation" indicates the registration errors of the proposed method without geometric constraints (i.e., Formula 5). The experiments are implemented in C++ on a computer with 16 GB RAM and an Intel Core i7-4850HQ @2.3GHz CPU.

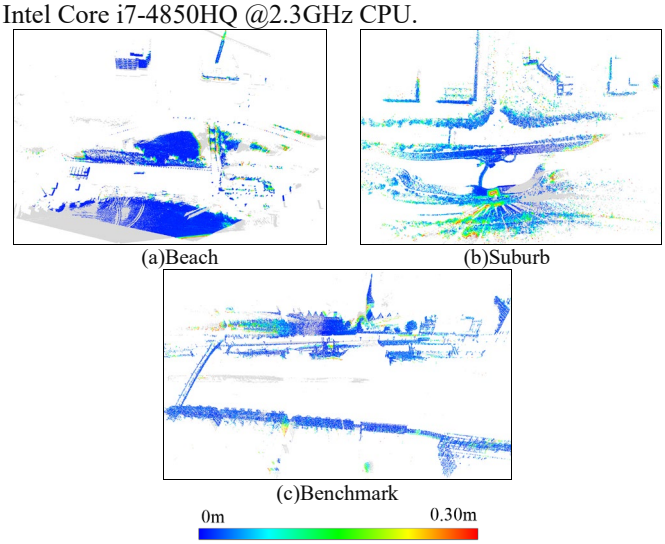

Figure 4. Registration errors of the three datasets. Different colors represent different degrees of registration errors.

TABLE II
EVALUATION OF REGISTRATION PERFORMANCE.

Datasets	Avg. error (m)		RMSE (m)		Iterations	Runtime
	proposed	ablation	proposed	ablation		
Beach data	0.053	1.25	0.034	0.49	36	440s
Suburb data	0.12	34.40	0.087	9.27	41	459s
Benchmark	0.081	0.096	0.048	0.012	27	308s

Figure 4 shows that all three datasets are aligned well, and that registration errors are evenly distributed. Figure 4 (b) shows much higher errors through. This is because the presence of vegetation affects feature estimation and matching probabilities. From TABLE Ⅱ, we can see that the registration errors are controlled efficiently. All registration errors are about 0.1m, and the RMSE is controlled within 0.1m. Compared to the ablation experiments, the proposed method outperforms the registration method without geometric constraints, demonstrating its robustness and effectiveness. These registration results can be improved further by local registration (e.g., ICP). In addition, the iterations and runtime show its fast convergence (e.g., the number of iterations is about 40). This demonstrates the efficiency and robustness of the proposed method.

C. Evaluation of Correspondences Determination

To show the matching performance of the proposed method directly, we select the 200 correspondences of highest matching probability for each iteration. Figure 5 shows the correspondence determination of the different iterations of the Suburb data.

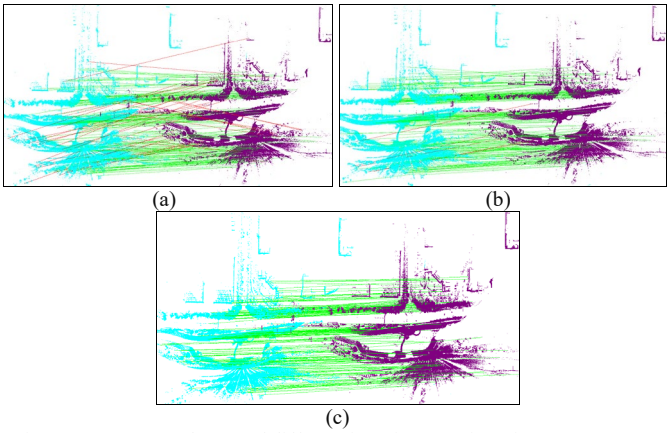

Figure 5. Correspondences of different iterations: (a) iteration 1, 133 correct matches; (b) iteration 10, 193 correct matches; (c) iteration 20, 200 correct matches (blue points indicate the left station, the purple points indicate the right station, green lines indicate correct matches, while red the mismatches).

As can be seen in Figure 5, an increasing number of correct matches is determined within a few iterations. This is because the geometric and structural constraints reject outliers efficiently, showing the superiority of matching. Since all correspondences directly contribute to the transformation, this correspondence determination model used by our method has succeeded in pinpointing correct matches in a seemingly un-structural point cloud.

D. Comparison to Other Methods

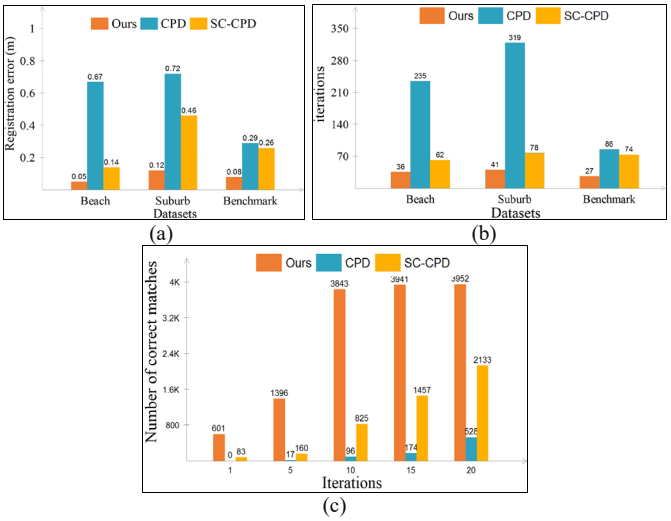

Figure 6. Comparison to other methods: (a) registration errors; (b) iterations for convergence; (c) number of matches at different iterations.

Since the initial point clouds are too big for CPD and SC-CPD, we use Geomagic Studio 2012 to uniformly down-

sample the point clouds before applying these methods. Figure 6 shows the performance of the proposed method compared to other methods. The suburb data is used in Figure 6(c).

Figure 6(a) shows that the proposed method has better accuracy compared to the other two methods. Figure 6(b) shows that the proposed method requires fewest iterations for convergence. This is because the simplification mitigates the influence of density variations, and the probabilistic model incorporates efficient geometric constraints and structural information, improving the performance significantly. Figure 6(c) shows that the proposed method has higher number of correct matches at different iterations, indicating its improved performance in correspondence determination. This demonstrates the robustness and efficiency of this probabilistic method.

IV. CONCLUSION

In this letter, we propose a global registration method based on the CPD framework for TLS point clouds. Three components have been introduced to improve the robustness and efficiency of the original CPD algorithm. For point cloud simplification, the measurement geometry and the intrinsic characteristics of the scene are incorporated together to reduce the influence of density variation. We incorporated geometric information as well as structural constraints in the probabilistic model to improve the robustness of matching. A spectral graph is used to measure the structure similarity of matching points at each iteration. Experiments were conducted on three real datasets, showing the effectiveness and efficiency of the proposed method. It could also be shown that the proposed method significantly outperforms state-of-the-art methods in terms of alignment accuracy and robustness.

Although the proposed method has achieved promising results, there still space for improvement. For example, the features used are sensitive to vegetation as incorrect matches may be introduced. A novel and robust descriptor for cluttered scenes deserves future research.

REFERENCES

[1] L. J. Sánchez-Aparicio, S. Del Pozo, L. F. Ramos, A. Arce, and F. M. Fernandes, "Heritage site preservation with combined radiometric and geometric analysis of TLS data," *Automation in Construction*, 85: 24-39, 2018.

[2] Z. Li, L. Zhang, P. T. Mathiopoulos, F. Liu, L. Zhang, S. Li, and H. Liu, "A hierarchical methodology for urban facade parsing from TLS point clouds," *ISPRS Journal of Photogrammetry and Remote Sensing*, 123: 75-93, 2017.

[3] H. Lei, G. Jiang, and L. Quan, "Fast descriptors and correspondence propagation for robust global point cloud registration," *IEEE Transactions on Image Processing*, 26(8): 3614-3623, 2017.

[4] Y. Chen, and G. Medioni, "Object modeling by registration of multiple range images," *Image and vision computing*, 10(3): 145-155, 1992.

[5] P. J. Besl, and N. D. McKay, "Method for registration of 3-D shapes," *Proc. SPIE*, vol. 1611, no. 1, pp. 586-606, Apr. 1992.

[6] P. Mavridis, A. Andreadis, and G. Papaioannou, "Efficient sparse icp," *Computer Aided Geometric Design,* 35: 16-26, 2015.

[7] F. Pomerleau, S. Magnenat, F. Colas, M. Liu, and R. Siegwart, "Tracking a depth camera: Parameter exploration for fast ICP," *IROS*, 2011, September, pp, 3824-3829, 2011.

[8] H. Hong, and B. H. Lee, "Probabilistic normal distributions transform representation for accurate 3d point cloud registration," In: *2017 IEEE/RSJ IROS. IEEE*, pp, 3333-3338, 2017.

[9] D. Campbell, and L. Petersson, "An adaptive data representation for robust point-set registration and merging," In: *Proceedings of the IEEE ICCV*. pp. 4292-4300, 2015.

[10] P. Kim, J. Chen, Y. K. Cho, "SLAM-driven robotic mapping and registration of 3D point clouds," *Automation in Construction*, 89: 38-48, 2018.

[11] Z. Kang, F. Jia, and L. Zhang, "A Robust Image Matching Method based on Optimized BaySAC," *Photogrammetric Engineering & Remote Sensing*, 80(11): 1041-1052, 2014.

[12] Z. Kang, J. Li, L. Zhang, Q. Zhao, and S. Zlatanova, "Automatic Registration of Terrestrial Point Clouds using Reflectance Panoramic Images," *Sensors*, 9(4): 2621-2646, 2009.

[13] D. Fontanelli, L. Ricciato, and S. Soatto, "A fast ransac-based registration algorithm for accurate localization in unknown environments using lidar measurements," In *2007 IEEE of CASE*, pp. 597-602, 2007.

[14] D. Aiger, N. J. Mitra, and D. Cohen-Or, "4-points congruent sets for robust pairwise surface registration," In *ACM TOG*, 27(3):85, 2008.

[15] A. Myronenko, and X. Song, "Point set registration: Coherent point drift," *IEEE transactions on pattern analysis and machine intelligence*, 32(12): 2262-2275, 2011.

[16] D. A. Lachinov, A. A. Getmanskaya, and V. E. Turlapov, "Refinement of the Coherent Point Drift Registration Results by the Example of Cephalometry Problems," *Programming and Computer Software*, 44(4): 248-257, 2018.

[17] P. Wang, P. Wang, Z. Qu, Y. Gao, and Z. Shen, "A refined coherent point drift (CPD) algorithm for point set registration," *Science China Information Sciences*, 54(12): 2639-2646, 2011.

[18] L. Peng, G. Li, M. Xiao, and L. Xie, "Robust CPD algorithm for non-rigid point set registration based on structure information," *PloS one*, 11(2): e0148483, 2016.

[19] F. J. Lawin, M. Danelljan, F. S. Khan, P. Forssén, and M. Felsberg, "Density Adaptive Point Set Registration," *2018 IEEE Conference on CVPR*, 3829-3837, 2018.

[20] S. Soudsarissanane, "The Geometry of Terrestrial Laser Scanning, Identification of Errors, Modeling and Mitigation of Scanning Geometry," Ph.D. Thesis, Delft University of Technology, Delft, The Netherlands, 2016.

[21] M. Weinmann, M. Jutzi, S. Hinz, and C. Mallet, "Semantic point cloud interpretation based on optimal neighborhoods, relevant features and efficient classifiers," *ISPRS Journal of photogrammetry and remote sensing*, 105, 286-304, 2015.

[22] Z. Dong, B. Yang, Y. Liu, F. Liang, B. Li, and Y. Zang, "A novel binary shape context for 3D local surface description," *ISPRS Journal of Photogrammetry and Remote Sensing*, 130, 431-452, 2017.

[23] B. He, Z. Lin, and Y. Li, "An automatic registration algorithm for the scattered point clouds based on the curvature feature," *Optics & Laser Technology*, 46, 53-60, 2013.

[24] B. Yang, Y. Zang, Z. Dong, and R. Huang, "An automated method to register airborne and terrestrial laser scanning point clouds," *ISPRS Journal of photogrammetry and remote sensing*, 109: 62-76, 2015.

This work was supported in part by the National Science Foundation of China project under Grant 41701529, and University Science Research Project of Jiangsu Province under Grant 17KJB420004, and OpenFund of State Laboratory of Information Engineering in Surveying, Mapping and Remote Sensing, Wuhan University under Grant 18S02, and in part by the National key technology support program under grant 2014BAL05B07. (*Corresponding author: Yufu Zang.*)

1. Y. Zang and H. Guan are with School of Remote Sensing & Geomatics Engineering, Nanjing University of Information Science & Technology, Nanjing 210044, China (e-mail: 3dmapzangyufu@nuist.edu.cn).

2. Y. Zang and R. Lindenbergh are with the Department of Geoscience and Remote Sensing, Delft University of Technology, 2628 CN Delft, The Netherlands.

3. B. Yang is with the State Key Laboratory of Information Engineering in Surveying, Mapping, and Remote Sensing, Wuhan University, Wuhan 430079, China.